

New Materials for High Temperature Thermoelectric Power Generation

Reactor Concepts

Susan Kauzlarich

University of California, Davis

Dirk Cairns-Gallimore, Federal POC
Stephen Johnson, Technical POC

ANNUAL PROGRESS REPORT

Project Title: *New Materials for High Temperature Thermoelectric Power Generation CFP-12-3714 MS-RC2: Space and Defense RD&D Radioisotope Thermal Generator Technologies*

Covering Period: Final Report, January 1, 2013 -December 31, 2015

Date of Report: January 16, 2016

Recipient: University of California, Davis
One Shields Ave
Davis, CA 95616

Award Number: NEUP 12-3714

Principal

Investigator: Susan Kauzlarich, 530-752-4756, smkauzlarich@ucdavis.edu

Project Objective: The scope of this proposal was to develop two new high ZT materials with enhanced properties for the n- and p-leg of a thermoelectric device capable of operating at a maximum temperature of 1275 K and to demonstrate the efficiency in a working device. Nanostructured composites and new materials based on n- and p-type nanostructured $\text{Si}_{1-x}\text{Ge}_x$ ($ZT_{1273\text{K}} \sim 1$) and the recently discovered p-type high temperature Zintl phase material, $\text{Yb}_{14}\text{MnSb}_{11}$ ($ZT_{1273\text{K}} \sim 1$) were developed and tested in a working device.

Task 1. $\text{Si}_{1-x}\text{Ge}_x$ nanocomposite.

Summary: N-type YbP/ $\text{Si}_{95}\text{Ge}_5$ composite alloys were synthesized via mechanical alloying of Si, Ge, YbH_2 and P. The sintered samples are dense pellets and thermoelectric properties were fully characterized. YbP tunes carrier concentration but did not lower the thermal conductivity. This might be attributed to problems with achieving uniform particle size. The deviation of up to 25 % between different instruments set up of Seebeck measurements were noticed and is attributed to the differences in metal alloy for the thermocouples. Using the most conservative Seebeck measurements, the highest zT is about 0.7 at 1275 K.

The n-type nanostructured $\text{Si}_{1-x}\text{Ge}_x$ was investigated to determine whether thermal conductivity could be preferentially reduced by means of preparing a nanocomposite in situ utilizing a metal hydride. Phosphorus doped $\text{Si}_{95}\text{Ge}_5$ was chosen as the starting place for the systematic investigation as this material has been reported with zT's as high as 1 in the high temperature leg. The application of a ytterbium hydride to prepared Yb_2Si was the initial goal. It was determined that YbP rather than Yb_2Si was formed. Initially this result led to low carrier concentrations because the YbH_2 starting material was simply reacting with the phosphorus dopant. We determined that this was happening through careful microprobe and TEM analysis. Therefore, we focused the final year on optimizing the YbP- $\text{Si}_{95}\text{Ge}_5$ composite. The

carrier concentration of the samples were controlled by the amount of YbH_2 added, removing some of the phosphorus to form YbP. *N*-type $\text{Si}_{95}\text{Ge}_5$ alloys with higher YbP composite amount showed lower electrical thermal conductivity but not the expected lower lattice thermal conductivity. The 2 % YbP contained SiGe sample achieved zT of 0.67 at 1274 K. Another series of *n*-type $\text{Si}_{95}\text{Ge}_5$ alloys with YbP purposely synthesized with additional P compositions (0, 1, 2 %) to compensate the dopants loss from YbP formation. The thermoelectric properties were characterized from room temperature to 1273 K, and the samples possess electrical resistivity and carrier concentrations as expected from the additional P dopant. However, with similar charge carrier concentrations, the presence of YbP did not lower lattice thermal conductivity effectively. While we were able to reproduce results with JPL, there are significant difference in Seebeck measurements between our data collection and theirs. This problem was not resolved and deserves further investigation. The UCD results are more consistent with related literature, but the JPL resulted suggested a lower Seebeck coefficient and this report provides the JPL results in order to be conservative. Therefore the as made *n*-type SiGe sample has a peak zT of 0.57 at 1200 K.

Table 1 provides the sintered pellets that were used in the transport and thermal conductivity measurements.

Table 1. Measured density (g/cm^3) of sintered $\text{Si}_{95}\text{Ge}_5$ pellets¹ at room temperature.

$\text{Si}_{95}\text{Ge}_5$ Sample	No YbH_2	1 % YbH_2	2 % YbH_2	5 % YbH_2	* No YbH_2	* 1 % YbH_2	* 2 % YbH_2
Density (g/cm^3)	2.48	2.56	2.72	2.45	2.41	2.59	2.67

¹All samples were prepared with 3% P dopant. The samples indicated with * had addition P added in an equivalent % as the YbH_2 .

The XRD patterns of the first four samples indicated in Table 1 are shown in Figure 1. The series of samples indicated by * in Table 1 gave similar XRD patterns. $\text{Si}_{95}\text{Ge}_5$ is the main phase with YbP apparent and indicated by the lines in Figure 1. The relative diffraction intensity of YbP increases with the YbH_2 concentrations. There are additional phases in the 5 % YbH_2 containing sample possibly from oxide phases when excess Yb is present.

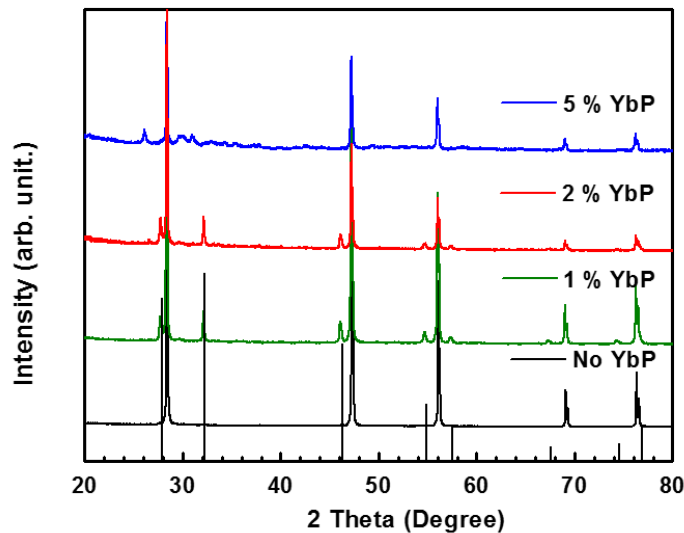


Figure 1. X-ray diffraction pattern of sintered n type $\text{Si}_{95}\text{Ge}_5$ pellets indexed with YbP phases by the drop lines.

Figure 2 shows the electrical resistivity of composite YbP/ $\text{Si}_{95}\text{Ge}_5$ samples from 275 K to 1273 K. the first series of samples shows that by 5% YbP, the electrical resistivity is too high for the sample to be of interest. The second series were prepared in a slightly different manner, but show remarkable consistency with the first set. The high temperature data between 800-1100 K show an unusual temperature dependence that was reproducible but we did not determine its origin.

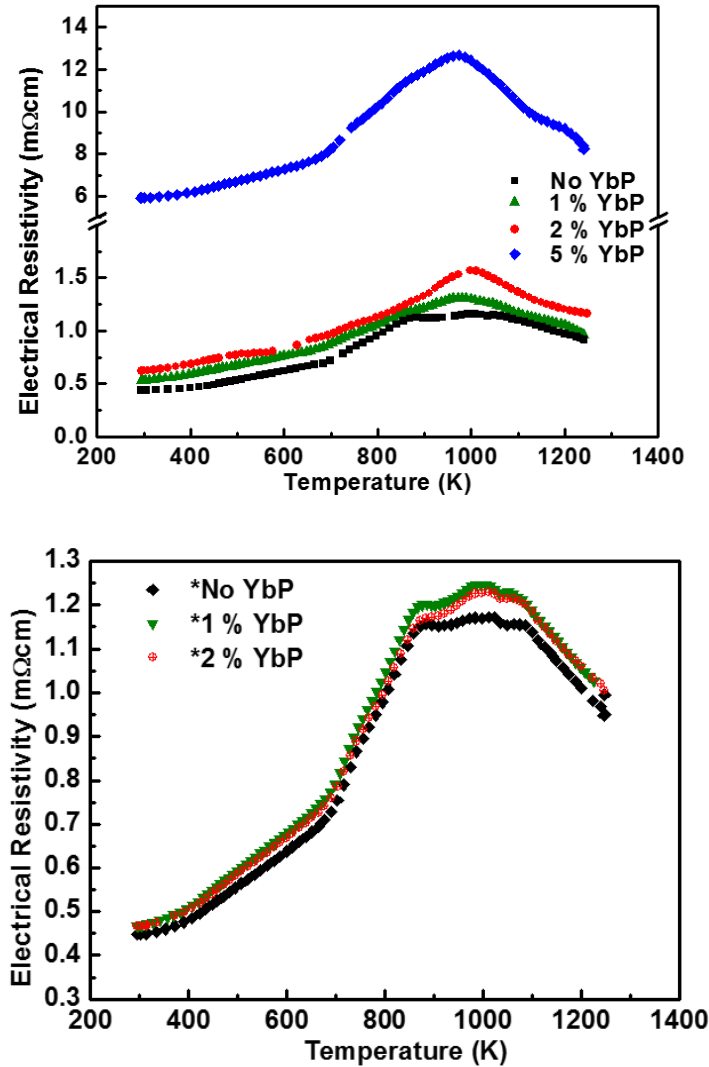


Figure 2. Electrical resistivity of n type $\text{Si}_{95}\text{Ge}_5$ samples measured from 275 K to 1273 K. Electrical resistivity of four samples with same P dopants (3 a.t. %) are presented in upper figure and the three * samples with additional P dopants are presented in the lower figure.

Figure 3 shows carrier concentrations as well as mobility from 275 K to 1273 K. The samples are heavily doped n type semiconductor with electron carrier concentration in the range of $2 \times 10^{20} \sim 5 \times 10^{20} \text{ cm}^{-3}$ at room temperature. The samples' mobility are in the same range, about $30 \text{ cm}^2/\text{Vs}$

at room temperature, with the exception of the 5 % YbP sample. All the samples possess linearly decreased mobility with increased temperature.

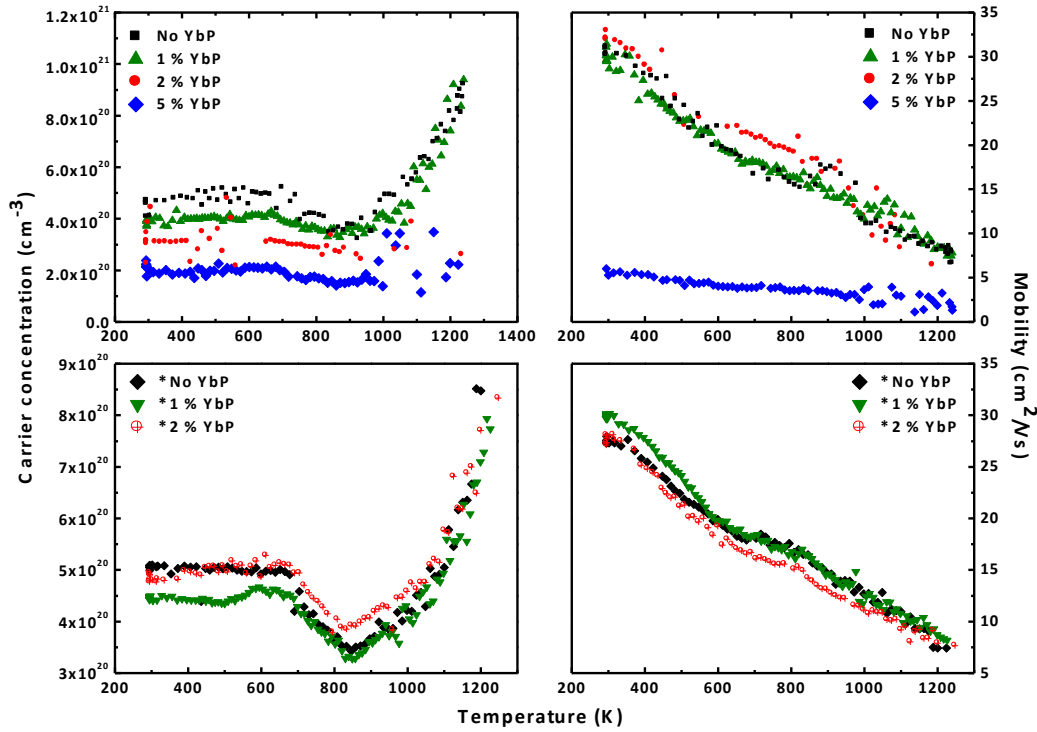


Figure 3. Charge carrier concentrations and mobility from Hall measurements in the temperature range of 275 K to 1275 K.

Figure 4 shows the Seebeck measurements. The JPL group measures their samples in a custom built uniaxial set-up and the UCD group uses a commercial four probe off axis set up.

In the uniaxial set up, absolute Seebeck coefficient was measure from 275 K to 1200 K under vacuum. Samples showed large negative Seebeck coefficients from about $-60 \mu\text{V/K}$ at 275 K and their absolute Seebeck coefficients increased with temperature until around 1000 K above which it bent over. The decreased absolute Seebeck coefficients are consistent with the increased carrier concentrations according to the Pisarenko relation. The Seebeck coefficients of the two series of samples are shown in the upper and lower figures separately. The SiGe sample with 2 % YbP content from the first series of samples showed a maximum absolute Seebeck coefficient value of over $|-200| \mu\text{V/K}$ at about 1000 K, while no YbP and 1 % YbP content samples' Seebeck coefficient are in similar range and stay below $|-200| \mu\text{V/K}$. The YbP composites influence Seebeck coefficient by tuning the charge carrier concentration. In the second series of samples, the samples with 1 % and 2 % YbP content possess Seebeck coefficient in the same range and the sample with no YbP have slightly higher absolute Seebeck coefficient value. The samples were cut and measured again with an off axis set up instrument to compare and verify the results. And the measurement results are plotted in the same graph with the uniaxial set up measurement results. The Seebeck coefficient measurements showed inconsistent results as the off axis measurement gave overestimated Seebeck coefficient of up to 25 % higher than at

1000 K than the results from uniaxial Seebeck coefficient. Compare the two set up of Seebeck coefficient measurements, one of the main differences is the position of thermocouples which measure temperature and voltage simultaneously. The Seebeck coefficient is obtained from $\Delta V/\Delta T$, therefore, the accurate reading of temperature from thermocouples is critical for Seebeck coefficient measurements.¹²

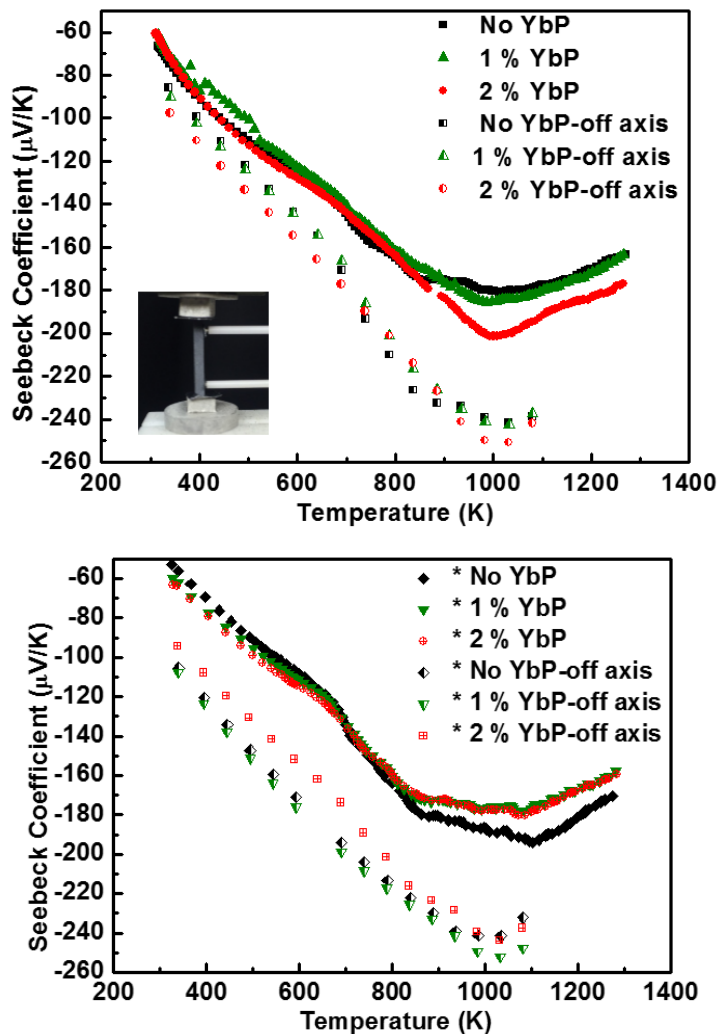


Figure 4. Comparisons of Seebeck coefficients measurements results from uniaxial instrument set up and off axis set up on the same samples. The photo of the off axis set up of instrument with sample in place is shown in the upper graph.

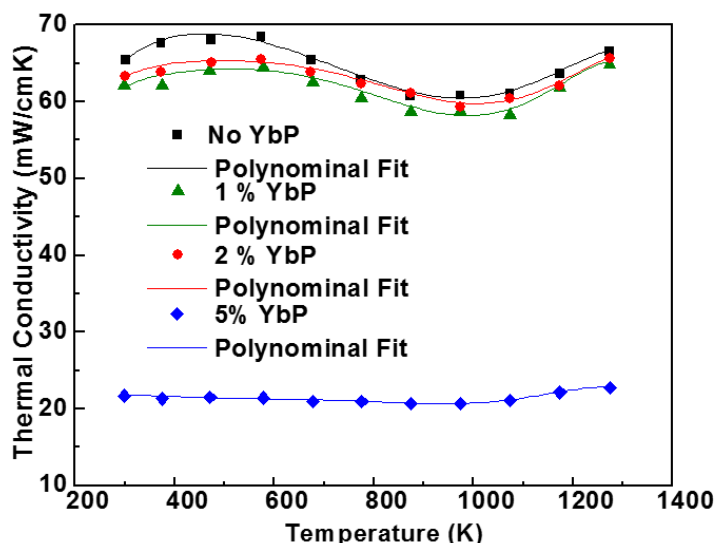
In the off axis set up, the sample bars are clamped in between the Pt electrodes, and two Pt thermocouples are pressed against the sample off axis. The measurement was performed under helium and graphite foils was used in between the sample and Pt electrodes to prevent the reaction at high temperature. It was noticed as the thermocouples are off axis from the heating source and the thermocouples extend to the electronic parts outside the furnace, which stay about room temperature. The thermocouples can act as cold fingers at the contact position with the sample and disturb temperature gradient reading. The reading could be underestimated and therefore the Seebeck coefficients are overestimated.^{14, 15}

In the uniaxial set up, the thermocouples are embedded through the heater and cold finger effect can be resolved, but as the thermocouples are in contact with the samples by constant pressure independently, the strength of the two thermocouples towards the sample can still affect the temperature reading.¹⁵

This disagreement of Seebeck coefficient measurement results from different instrumental set up is not seen in report of the thermoelectric characterization of $\text{Yb}_{14}\text{MnSb}_{11}$, on which similar experimental procedures were performed and the Seebeck coefficient results were consistent.¹⁶ Compare these two thermoelectric studies, $\text{Yb}_{14}\text{MnSb}_{11}$ with a large complex unit cell, possess thermal conductivity about ten times smaller than SiGe alloys.¹⁶ It is possible that the cold effect influences Seebeck coefficient measurement more on compounds with high thermal conductivity than the compounds with low thermal conductivity. As the off axis set up of Seebeck coefficient measurements are common in commercial instruments (ZEM, Linseis, *etc.*), researchers should raise awareness of this temperature reading deviation in the Seebeck coefficient measurements of the SiGe alloys.

The thermal conductivity of the SiGe samples was characterized from 275 K to 1275 K and plotted in Figure 5. The samples possess moderate thermal conductivity in the range of about 60 ~ 70 mW/cmK. Compare the thermal conductivity with what have been reported in the literature, it is lower than the bulk $\text{Si}_{95}\text{Ge}_5$ which have the same low Ge content, but higher than $\text{Si}_{80}\text{Ge}_{20}$ alloys used in RTG.^{6,9}

To examine the influence of YbP composites on the lattice thermal conductivity, the electrical thermal conductivity were calculated with the Wiedemann-Franz equation, $\kappa = LT/\rho$, in which the measured electrical resistivity at the same temperature range was used. The lattice thermal conductivity was estimated by subtracting electrical thermal conductivity from the total thermal conductivity and is shown in Figure 6.



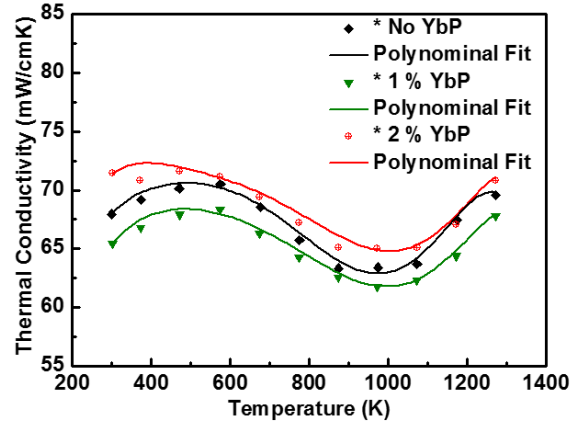


Figure 5. Thermal conductivity results from laser flash measurements on the 12.7 mm pellets.

In the first series of SiGe samples, the total thermal conductivity decrease with YbP content. After estimating the electron and phonon contributions to the total thermal conductivity, the YbP composites influence the thermal conductivity by decreasing the electron carrier concentrations but not decreasing the lattice thermal conductivity since the sample with no YbP showed slightly lower lattice thermal conductivity. In the second series of samples, the total thermal conductivity from measurement as well as the estimated lattice thermal conductivity have very similar values. Unfortunately the phases with YbP did not lower the lattice thermal conductivity as expected.

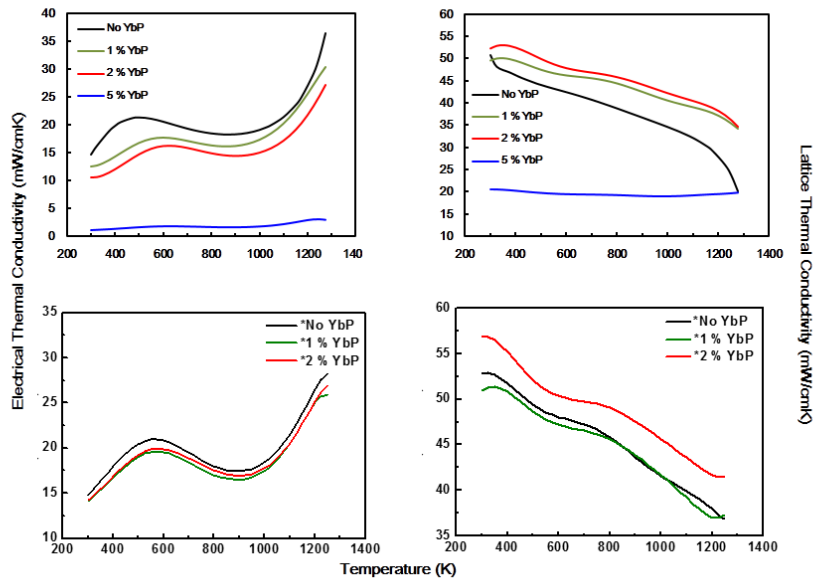


Figure 6. The electrical thermal conductivity of the two series of samples are estimated with Wiedemann-Franz equation, and lattice thermal conductivity is shown on the right side after subtracting electrical thermal conductivity from the total thermal conductivity.

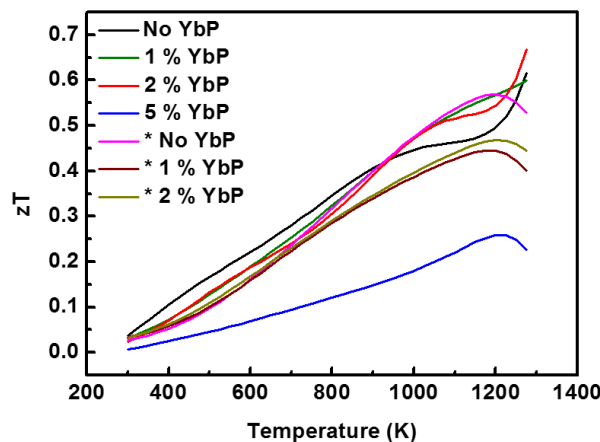


Figure 7. The figure of merit of n-type YbP/Si₉₅Ge₅ composite samples.

The figure of merit of SiGe alloys were calculated from the polynomial fits of measured electrical resistivity, Seebeck coefficient (from uniaxial instrumental set up) and thermal conductivity. The SiGe samples from the first series of samples (no additional P dopants) with no YbP (in Black line), 1 % YbP (in Green line) and 2 % YbP (in Red line) showed zT increasing with temperature. 2 % YbP content sample showed highest zT among the all samples which is close to 0.7 at 1273 K. As the thermoelectric properties are interrelated by carrier concentration, the enhancement of thermoelectric properties is attributed to the improved absolute Seebeck coefficient and lower thermal conductivity, mainly from decreased carrier concentration. Compared to n type Si₈₀Ge₂₀ alloys which has peak zT of 1 in the temperature range of 900 to 950 °C, the low Ge content SiGe samples possess lower figure of merit, because YbP inclusions in the matrix failed to decrease the thermal conductivity as expected and with less Ge, the absolute Seebeck coefficient decreases. The zT of samples with additional P bend over when temperature exceeding 1200 K. The * sample with no YbP composite possess a peak zT of 0.57 at 1200 K, comparable to the 2 % YbP contained SiGe sample at the similar temperature range. The YbP composite in the * samples doesn't enhance thermoelectric performance of the SiGe matrix.

Task 2. Synthesis of variants of Yb₁₄MnSb₁₁.

Summary: A number of new variants were explored: Yb_{14-x}RE_xMnSb₁₁, RE = Sc, Y, Ce, Pr, Sm; $x = 0.1, 0.2, 0.3, 0.4, 0.5, 0.6, 0.7, 0.8$; Yb₁₄MnSb_{11-x}Se_x; Yb₁₄MnBi₁₁; Yb_{14-x}Ca_xMnBi₁₁; Yb₁₀Ca₃BiMnSb₁₁; Yb₁₄MgSb₁₁. These samples were fully characterized and validated with measurements at both UCD and JPL. After survey measurements in years 1-2, year 3 focused on Yb₁₄MgSb₁₁ with the goal of metallization and leg testing. The Yb₁₄MgSb₁₁ was scaled to 100g and successfully reproduced the original UC Davis results. The material was successfully bonded to the hot shoe with good adhesion and limited diffusion. The device couple is shown below.

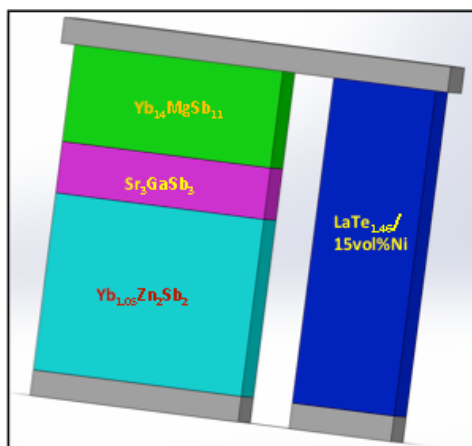


Figure 8. A device couple, using all Zintl phases for the p-leg and $\text{LaTe}_{1.46}$ for the n-leg.

Figure 8 shows the device couple that is in the process of being tested at JPL. The overall couple level $zT \sim 1.11$ and the projected efficiency is 14%. This is the first demonstration of a p-leg for all Zintl materials segmented leg. $\text{Yb}_{14}\text{MgSb}_{11}$ was chosen for the high temperature segment because of better compatibility with minimal sublimation and good engineering match to the other materials.

Publications:

1. Kawamura, Airi; Hu, Yufei; Kauzlarich, Susan M. "Synthesis and Thermoelectric Properties of the YbTe-YbSb System". *Journal of Electronic Materials*, **45**(1), 2016, 779-785, DOI: 10.1007/s11664-015-4202-x
2. Grebenkemper, Jason H.; Hu, Yufei; Barrett, Dashiell; Gogna, Pawan; Huang, Chen-Kuo; Bux, Sabah K.; Kauzlarich, Susan M. "High Temperature Thermoelectric Properties of $\text{Yb}_{14}\text{MnSb}_{11}$ Prepared from Reaction of MnSb with the Elements" *Chemistry of Materials*, **27** (16), 2015, 5791-5798, DOI: 10.1021/acs.chemmater.5b02446
3. Hu, Yufei; Wang, Jian; Kawamura, Airi; Kovnir, Kirin; Kauzlarich, Susan M. $\text{Yb}_{14}\text{MgSb}_{11}$ and $\text{Ca}_{14}\text{MgSb}_{11}$ -New Mg-Containing Zintl Compounds and Their Structures, Bonding, and Thermoelectric Properties" *Chemistry of Materials*, **27**(1), 2015, 343-351, DOI: 10.1021/cm504059t
4. Hu, Yufei; Bux, Sabah K.; Grebenkemper, Jason H.; Kauzlarich, Susan M. "The effect of light rare earth element substitution in $\text{Yb}_{14}\text{MnSb}_{11}$ on thermoelectric properties" *Journal of Materials Chemistry C*, **3**(40), 2015, 10566-10573, DOI: 10.1039/c5tc02326b